Design of Steel Column Using LRFD Method

Mohamed A. A. El-Shaer

Civil and Construction Engineering Department, Higher Technological Institute, 10th of Ramadan City
ecg_group@yahoo.com

Abstract: In this paper a procedure for designing column with slender sections was established. A column design curve for slender sections was established by applying a reduction factor, Q, to the LRFD column design curve. A stability analysis was conducted to study the effect of plate local buckling on flexural column buckling. A finite element model of an axially loaded I-column was developed using shell elements. Material and geometric nonlinearities were incorporated. Geometric imperfections similar to the first buckling mode with amplitude of 1/775 of column length, L, were applied. The analysis was carried out using the general purpose finite element program ANSYS. A wide range of plate width-to-thickness ratios and column slenderness ratios was studied. Column sections were grouped into three Groups: Group 1; sections with slender unstiffened plate elements, Group 2; sections with slender stiffened plate elements, and Group 3; sections composed of slender stiffened and unstiffened elements. The buckling loads for 144 I-column configurations made of steel 37, 44 and 52, and were compared to respective values adopted by the AISC-LRFD and Euro-Code3 specifications.
[Mohamed A. A. El-Shaer **Design of Steel Column Using LRFD Method]** Life Science Journal,. 2011; 8(4): 205-220] (ISSN: 1097-8135). http://www.lifesciencesite.com

Keywords: Column, Steel, LRFD, Finite elements.

1. Introduction

The load carrying capacity of compression members composed of slender plate elements is probably less than the overall buckling strength based on the slenderness ratio of the entire cross-section. This is because local buckling may occur in one of the plate elements that make up the cross-section. Therefore, the buckled element will not support its proportionate share of column load, thus the cross-section efficiency is reduced [1].

It is evident that studying the buckling of uniformly compressed plates is essential for the determination of column load when slender plate elements are used. A brief description of previous research work established to determine the bucking resistance of columns with thin-walled elements is presented in the following sections.

1.1 Behavior of Plates under Edge Compression:

The behavior of plates in compression is similar to columns and the basic elastic buckling stress for plates corresponding to Euler equation for columns was derived [1,2] as:

$$Fcr = k\pi^2E/\{12(1-\mu^2)(b/t)^2\} \quad (1)$$

Where k is plate buckling coefficient depending on boundary conditions and loading configuration, μ is Poisson's ratio, E is the elastic modulus, b is the plate width and t is the plate thickness. Examination of critical stress recorded from experiments showed that for low b/t ratios, strain hardening is achieved and F_{cr} exceeds the yield stress, F_y. The actual strength of plates for large b/t ratios exceeds F_{cr} given by Equation (1), i.e. they exhibit post-buckling strength.

1.2 Post Buckling Strength and Effective Width of Plates:

When a thin plate is axially loaded, it will buckle in regular waves when the stress reaches F_{cr}, but it will not collapse due to material ductility. If plate edges parallel to load were kept straight by supports, the plate will exhibit post-buckling strength. The central portion of the plate will exhibit excessive lateral deflections with increasing load and can hardly participate in carrying the load. Stresses will be continually redistributed so that stresses are increasing at edges and kept almost constant at the central portion. The resulting non-uniform stress distribution can thus be replaced by an equivalent uniform stress applied on an effective width of the plate. The post-buckling strength of plates was first described [3] by the effective width concept introduced by **Dawson and Walker** in **1972**. Both the American and British design specifications for cold-formed sections adopted a semi-empirically computed effective width to describe the post buckling behavior of plates.

A generalized imperfection parameter written in terms of F_y and F_{cr} was used in the derived expressions. Results were confirmed by comparison with test data. **Lind *et al.*** [4] reviewed the data basis for the effective width formulas used in slender sections design. A simple effective width formula that yields correct results in view of experimental evidence rather than mechanical analysis was introduced based on statistical approach. Results were adopted by the **Canadian**

standard S-146 (1974). **Horne and Narayanan** [5] established a design method for stiffened slender plates subjected to compression. Usami [6] studied the problem of elastic post-buckling behavior of plates in combined compression and bending.

1.3 Elastic and Inelastic Buckling of Plates:

Lind [7] established a numerical procedure to compute the elastic local buckling load of plate assemblies by solving an eigen value problem of an ordinary differential equation by the Newmark numerical approach. The method is applicable to slender sections subjected to constant compressive force and moment. **Sherbourne and Korol** [8] showed that upper bound of plates buckling load in the intermediate stage of elastic-plastic interaction for moderate b/t ratios can be determined by the intersection of plastic mechanism with elastic post-buckling strength. The accuracy of such estimate was verified by comparison with test data that showed that buckling load in the inelastic range was slightly dependent on imperfection amplitude. **Dawe *et al.*** [9] proposed a set of orthotropic material properties, derived semi-empirically for predicting inelastic buckling of stiffened and unstiffened plates. **Dawe *et al.,*** utilized the proposed orthotropic material properties in an analytical technique to predict the elastic and inelastic buckling load of hollow structural sections [10]. Effects of manufacturing process and interaction between adjacent plates were included in the formulation. Results were in good agreement with test data.

1.4 Numerical Buckling Analysis of Plate Assemblies:

The interaction between local and Euler buckling of thin-walled compression members was solved numerically by the finite element and finite strip methods. The finite element solution conducted by Gallagher incorporating material and geometric nonlinearities provided successful results in simulating nonlinear and post buckling behavior of plates. **Hancock** [11] extended the finite strip method to include the nonlinear membrane stiffness resulting from the interaction of geometric imperfections with local and post buckling phenomena of plates.

1.5 Design Specifications for Slender Compression Members:

For axially loaded compression members of cross sections having coincident shear center and centroid and composed of slender plate elements, the design strength, P_u, specified by the **AISC-LRFD** specifications [12] is given by:

$$P_u = \phi A_g F_{cr} \qquad (2)$$

$$\text{For } \lambda_c (Q)^{1/2} \le 1.5 \text{ , } F_{cr} = Q\,(0.658^{Q\lambda_c^2})\,F_y \qquad (3)$$
$$\text{For } \lambda_c (Q)^{1/2} > 1.5 \text{ , } F_{cr} = (0.877/\lambda_c^2)\,F_y$$

Where $\lambda_c = (Kl/r\pi)\,(F_y/E)^{1/2}$ column slenderness parameter based on gross section properties
(Kl/r)= Slenderness ratio of the column
Q = reduction factor to account for local buckling of slender plates
$= Q_a Q_s$
Q_a = reduction factor for stiffened elements.
Q_s = reduction factor for unstiffened elements.
ϕ = strength reduction factor for compression members, 0.85
A_g = gross cross section area

As discussed in Sec. 1.2, plate elements in compression possess post buckling strength. The AISC accounts for plate local buckling and post buckling strengths by applying the factors Q_a and Q_s is computed as the ratio of the effective area at a stress equal to ΦF_{cr} to the gross area of the cross section. The effective area is computed utilizing an effective width formula for stiffened elements based on Winter work [13].

The Euro-Code3 based on the **LRFD** approach [14] specifies the following design buckling resistance for compression members:

$$P_u = X\,\beta_a A_g F_y / \gamma_m \qquad (4)$$

Where β_a = 1, for compact and non-compact sections
= Effective area / gross area, for slender sections (corresponding to Q_a factor adopted in the AISC-LRFD)
γ_m = partial safety factor for buckling strength, 1.1
$X = 1/\{\phi + (\phi^2 - \beta_a \lambda_c^2)^{1/2}\} \le 1.0$
$\phi = 0.5[1 + \alpha\,\{\lambda_c (\beta_a)^{1/2} - 0.2\} + \beta_a \lambda_c^2]$
α = imperfection factor dependent on shape and axis of bending.

Similar to the AISC-LRFD, the Euro-Code3 accounts for local buckling of slender plate elements by introducing the reduction factor β_a based on the effective width concept. Unlike the AISC specifications, both stiffened and unstiffened elements are treated similarly by computing the effective width for a maximum edge stress equal to the material yield stress rather than the design compressive stress. Therefore the effective width computed by the Euro-Code will be conservative compared to the AISC and

will not require iterative solution.

Similar to the Euro-Code3, the Egyptian Code based on the allowable stress design, **ASD** [15] and **LRFD** [16] accounts for local buckling of slender plate elements by applying the effective width concept. The allowable compressive load, P_a, specified for members with slender plate elements composed of mild steel (St. 37) is given by:

$$P_a = A_{eff} F_{cr} \quad (5)$$

$$\text{For } l/r \le 100 \quad F_{cr} = 1.4 - 65x10^{-6} (l/r)^2 \ t/cm^2 \quad (6)$$
$$\text{For } l/r > 100 \quad F_{cr} = 7500/(l/r)^2 \ t/cm^2$$

Where l/r = governing slenderness ratio based on gross section properties.
A_{eff} = effective area based on effective width concept for stiffened and unstiffened plates.

The limit load computed was compared to the nominal buckling load adopted by the **AISC-LRFD** and Euro-Code3. Based on the study conducted herein, a set of design strength equations for columns composed of slender plate elements were established utilizing the effective width concept and the design strength formulas for non-compact members proposed by the same author [17].

2. Problem Description:

2.1 Geometric Configuration:

The column section considered herein is composed of an I-shaped section with flange and web width of 30 and 42 cm respectively. The column length, L, was assumed 3.0 m. Plate thicknesses were selected such that three Groups of slender sections were investigated. Group 1: sections composed of slender flanges at which C/t_f (Figure 1) exceeds $23/(F_y)^{1/2}$ [2] and non-compact web with d_w/t_w equals to $64/(F_y)^{1/2}$ [2]. Group 2: sections composed of slender web (i.e. d_w/t_w exceeds $64/(F_y)^{1/2}$) and non-compact flanges. Group 3: sections composed of slender flanges and web. Tables 1, 2 and 3 in Appendix A list the geometric configuration for Group 1, 2 & 3 sections considered; respectively.

2.2 Boundary Conditions:

Two boundary conditions configurations (Figure 1) were applied to mimic short and moderate length columns at which local plate buckling influences the column overall buckling. Case A; two hinged column with buckling length equals to L to represent short columns with small slenderness ratio. Case B; Fixed free column with buckling length of 2L to represent moderate columns with larger slenderness ratio. The slenderness ratio for each case based on section geometry and boundary conditions was listed in Tables 1, 2 & 3 in Appendix A.

2.3 Material Non Linearity:

A nonlinear stress-strain relation was adopted in the stability analysis to account for residual stresses [18]. The column strength curve adopted by the Column Research Council, CRC, was used with the tangent modulus theory to derive [17, 18] the stress-strain curve for steel 37, 44 & 52. Derivation of the adopted constitutive relation is illustrated in a previous research work by the same author [17]. The proportional limit stress, F_{pl}, was assumed equal to 0.5 F_y as per **CRC** [17, 18].

2.4 Geometric Imperfections:

Based on Koiter's buckling theory [17, 19, 3 & 11], an initial geometric imperfection having the shape of the first buckling mode of the perfect column was applied. Such imperfection configuration was used because it represents the worst possible imperfection that significantly affects the column load carrying capacity. The imperfection shape includes local buckling of thin-walled flanges and web.

3. Finite Element Modeling:

A finite element model for the column was constructed using **ANSYS** [20] shell elements. Flanges and web were modeled by plastic shell element, Shell43, in ANSYS element library. In order to incorporate material and geometric nonlinearities, the shell element selected possesses plastic, stress-stiffening and large deformation capabilities [20]. Figure 2 illustrates the three-dimensional column model used in the analysis. The first buckling mode was obtained for each column configuration by solving an Eigen-value problem by the general purpose finite element program, **ANSYS** [20]. An imperfection-amplitude of L/775 [17] was considered compared to an adopted value of L/1550 in the **AISC-LRFD** specifications [18]. Figure 3 illustrates the first buckling mode obtained for a column section of Group 1 with hinged-hinged boundary condition. Local buckling of thin-walled flange plates was dominant. However, if non-compact plate elements were used, a flexural half sine wave buckling mode about the minor axis would have been obtained.

4. ANALYSIS PROCEDURE:

A stability analysis was conducted to obtain the column limit load. The stability analysis is essentially a static analysis at which the column was loaded incrementally till failure. At each load step, equilibrium equations were solved iteratively till convergence was achieved by the modified **Newton-Raphson** technique [20,21]. Load increments were computed by the Arc-

Length option [20,21] to determine the limit load at which the column loses its stability. Non-uniform stress distribution was obtained during loading due to the existence of geometric imperfections and the application of non-linear material and geometry.

5. Comparison Of Finite Element Results With Specifications Designs:

The limit load stress obtained from the finite element solution for all column configurations studied herein was compared to the design compressive stress computed by the **AISC-LRFD** [12] and **Euro Code3** [14] specifications (Eqs 3 & 4 respectively). The following sections discuss the results obtained for sections of Groups 1, 2 & 3.

5.1 Sections of Group 1:

For sections of Group 1, C/t_f was varied from $0.7(E/F_y)^{1/2}$ to $1.15(E/F_y)^{1/2}$ whereas d_w/t_w was kept below the non-compact limit of $1.4(E/F_y)^{1/2}$. The ratio of flange area, A_f, to web area, A_w, ranged from 0.2 to 0.5.

Results indicated that in all cases the design compressive stress determined by AISC and Euro-code3 was less than FE results. Figures 4 and 5 depict the average computed compressive stress for each C/t_f ratio for short and medium columns respectively. Compressive stresses were normalized by the material yield stress. The AISC was more conservative than Euro-code3 when compared to FE results. For short columns, the design compressive stress recommended by the AISC was sharply reduced from 0.8 to 0.5 of FE limit load stress when C/tf was increased from $0.7(E/F_y)^{1/2}$ to $1.15(E/F_y)^{1/2}$ (see Fig 4). Similarly, for medium columns (Fig 5), the AISC design compressive stress was reduced from 0.90 to 0.75 of FE limit load as C/t_f increased. On the other hand, the Euro-Code3 recommended design compressive stress which took almost a constant value of 0.9 the FE limit load. This indicated that the AISC formulas overestimated the effect of local buckling on flexural buckling as C/t_f ratio increased and L/i ratio decreased.

5.2 Sections of Group 2:

For sections of Group 2, d_w/t_w was varied from $1.55(E/F_y)^{1/2}$ to $2(E/F_y)^{1/2}$ whereas the flange ratio C/t_f was kept below the non-compact limit of $0.5(E/F_y)^{1/2}$.Results indicated that both the AISC-LRFD and Euro-Code3 provided a good estimate of FE results. The ratio of design compressive stress computed by AISC-LRFD or Euro-Code3 was almost not affected by the variation in d_w/t_w ratio.

For short columns, the ratios of AISC-LRFD to FE and Euro-Code3 to FE results were almost constant with an average value of 0.90 and 0.93 respectively (Fig 6). Similarly, the ratios of AISC-LRFD and Euro-Code3 design compressive stress to FE results were constant, however, unlike short columns, the Euro-Code3 was slightly more conservative (Fig 7). This indicated that the recommended design compressive stress adopted by the Euro-Code3 and AISC-LRFD based on effective width concept was in good agreement with FE results.

5.3 Sections of Group 3:

For sections of Group 3, d_w/t_w was varied from $1.55(E/F_y)^{1/2}$ to $2(E/F_y)^{1/2}$ and for each value of d_w/t_w, the value of C/t_f was varied from $0.7(E/F_y)^{1/2}$ to $1.15(E/F_y)^{1/2}$. In most cases, the AISC-LRFD was more conservative than Euro-Code3 compared to FE results. It was noticed that the web width-to-thickness ratio had an insignificant effect on results. For short columns and similar to sections of Group1, the ratio of Euro-Code3 design compressive stress to FE limit load stress was almost constant with a mean value of 0.9 (Figs 4 & 8).

On the other hand, the design compressive stress recommended by the AISC-LRFD was sharply reduced from 0.9 to 0.5 of FE limit load stress (See Fig.8). A similar behavior was noticed for sections of Group 1 (Fig. 4). A similar behavior was noticed for medium columns, however, the AISC design compressive stress was in a better agreement with FE results (Fig 9). The ratio of AISC-LRFD design stress to FE limit load stress ranged from 0.9 to 0.7 when C/t_f increased from $0.7(E/F_y)^{1/2}$ to $1.15(E/F_y)^{1/2}$, whereas the ratio of Euro-Code3 design stress to FE limit load stress increased from 0.8 to 0.97.

The above discussion indicated that the AISC-LRFD overestimates local buckling effect on column buckling particularly for short columns with cross section containing slender unstiffened elements with high width-to-thickness ratio. This is mainly attributed to the application of the conservative stress reduction factor, Q_s (Sec. 1.5). The Euro-Code3, however, provided a better estimation of local buckling effect. In all cases, the effect of local buckling on the column carrying capacity is significantly reduced when slenderness ratio of the column increases and elastic buckling controls.

6. Column Design Curve For Members With Slender Plate Elements:

Based on the above discussion, the effective area approach adopted in the Euro-**Code3** [14] and **ECP-ASD** [15] specifications was adopted to account for the effect of slender plate local buckling on overall buckling of columns. The column design curve of compression members composed of slender plate elements was based on applying a reduction factor, Q, to the LRFD column curve proposed [17] for columns with non-compact sections. The reduction factor, Q is the ratio of the effective reduced area of the section,

A_{eff}, to the actual gross area, A_g. The effective width, b_e, of a slender plate is computed as per the **ECP-ASD 2010** [15] as follows:

$$b_e = \rho\, b \qquad (7)$$

Where
$$\rho = (\lambda_p - 0.20)/\lambda_p^2 \text{ if } \lambda_p > 0.673 \qquad (8\text{-a})$$
$$\rho = 1.0 \text{ if } \lambda_p \le 0.673 \qquad (8\text{-b})$$
$$\lambda_p = \{(b/t)\,(F_y/K)^{1/2}\}/44 \qquad (9)$$

b =appropriate flat width of slender plate element (Fig. 1)
= C for outstanding flanges
= d_w for webs
ρ = reduction factor to account for local buckling
λ_p = plate slenderness parameter
= $(F_y/F_{cr})^{1/2}$
F_{cr} = Elastic critical buckling stress of plates (Eq. 1) [7]K = plate buckling coefficient [7].
= 0.425, for uniformly compressed with unstiffened edges
= 4, for uniformly compressed plates with stiffened edges.

The effective width, b_e, is computed as follows:

$$b_e = 0.63\, t\,(E/F_y)^{1/2}\,[\,1\text{-}0.13\,(E/F_y)^{1/2}/(b/t)] \qquad (10)$$

Equation 10 is applicable to plate elements with unstiffened edges such as flanges, angles, and plates projecting from rolled or built-up sections of compression members. For plate elements with stiffened edges and substituting K by 4 in Eq. 9, b_e is computed as follows:

$$b_e = 1.92\, t\,(E/F_y)^{1/2}\,[\,1\text{-}0.385\,(E/F_y)^{1/2}/(b/t)] \qquad (11)$$

The design compressive load, P_u, of compression members with slender plate elements can be written as follows:

$$P_u = \phi\, A_g\, F_{cr} \qquad (12)$$

For $\lambda_c \le 1.1$ $\quad F_{cr} = Q\, F_y\,(1\text{-}0.384\,\lambda_c^2)$ (13)

For $\lambda_c > 1.1$ $\quad F_{cr} = 0.648\, Q\, F_y/\lambda_c^2$ (14)

Where
Q = A_{eff}/A_g
A_{eff} = effective area based on effective width of slender plate elements as per Eqs. 10 & 11.
ϕ = strength reduction factor,0.8.
λ_c = $(l/r\pi)\,(F_y/E)^{1/2}$ column slenderness parameter
l/r = governing slenderness ratio of the column.

The design compressive stress computed by Eqs 13 & 14 with the application of the strength reduction factor, ϕ,was compared to that computed by FE solution (Sec. 5), AISC-LRFD and Euro-Code3 in Tables 1, 2 & 3 (see Appendix A) for sections Groups 1, 2 & 3; respectively . The average design stress computed for each width-to-thickness ratio was also plotted for comparison in Figures 4 to 9.

7. Comparison of Proposed Column Ultimate Design Load Curve with Aisc-Lrfd Curve:

The ultimate load, P_u, computed by the proposed Eqs 12, 13 & 14 was compared to that obtained by the AISC-LRFD formulas for slender compression members. For Group 1 sections, the flange width to thickness ratio, C/t_f, was varied from $0.7(E/F_y)^{1/2}$ to $1.15\,(E/F_y)^{1/2}$. Since the reduction factor, Q, proposed herein is computed as the ratio of A_{eff} to A_g, it will be dependent on the ratio of the flange gross area to web gross area, A_f/A_w. Therefore, the factor A_f/A_w was varied from 0.1 to 0.5 to cover a wide range of practical cases. Figure 10 illustrates a comparison of column design curve computed by the proposed method (Eq 12) with that adopted by the AISC-LRFD (Eq 2). The comparison showed that for all values of C/t_f and A_f/A_w, the proposed equations are conservative compared to AISC-LRFD for long columns with $\lambda_c \ge 1.1$. This was attributed to the fact that the proposed column design formula adopts higher factor of safety for elastic buckling. On the other hand, the AISC-LRFD neglects the effect of local buckling in the elastic buckling region.

For columns with $\lambda_c \le 1.1$, the proposed method assumes higher design load compared to the AISC-LRFD especially for high values of C/t_f and A_f/A_w ratios. However, for $A_f/A_w \ge 0.4$ and $C/t_f \le 0.85\,(E/F_y)^{1/2}$, the proposed method is more conservative.

For Group 2 sections, the d_w/t_w ratio was varied from $1.55(E/F_y)^{1/2}$ to $2.0(E/F_y)^{1/2}$ whereas A_f/A_w was varied within the practical range of 1 to 4. Although the effective area approach is adopted in the proposed method and AISC-LRFD for Group 2 sections, comparison of design curves shows that the proposed method is more conservative with an average ratio of 0.92 for short columns and 0.68 for long columns (Fig. 11). This is attributed to the fact that the effective web width in the proposed method was based on the yield stress F_y (Eq. 11) whereas the AISC-LRFD uses the actual stress ϕF_{cr} in computing the effective width of unstiffened elements thus higher values of b_e will be provided. On the other hand, the proposed design curve is conservative in the elastic buckling range compared to the AISC-LRFD.

For Group 3 sections, the C/t_f ratio was varied from $0.7(E/F_y)^{1/2}$ to $1.15(E/F_y)^{1/2}$ whereas the d_w/t_w ratio was varied from $1.7(E/F_y)^{1/2}$ to $2(E/F_y)^{1/2}$ and A_f/A_w ratio was varied in the practical range of 0.5 to 2.0. The ratio of column ultimate design load curve determined by the proposed method to that adopted by the AISC-LRFD is illustrated in Fig 12. It is shown that the proposed design curve was conservative compared to AISC-LRFD for long columns with $\lambda_c \geq 1.1$. For short columns with $\lambda_c \leq 1.1$, the proposed method is also conservative compared to AISC-LRFD for sections with $C/t_f \leq 1.0\ (E/F_y)^{1/2}$.

8. Comparison of Proposed Column Ultimate Design Load Curve with Euro-Code3 Curve:

The proposed design curve is compared to Euro-Code3 column design curve based on the LRFD method. Since the Euro-Code 3 column design curve possess a flat plateau at small value of λ_c whereas the proposed design curve is parabolic, a noticeable reduction was observed in the ratio of the two design curves at λ_c equals 0.2 as shown in Figure 13.

Figure 13 depicts the column design curve for a wide range of C/t_f and A_f/A_w ratios. For Group 1 sections, comparison of design curves showed that the proposed method is always conservative compared to the Euro-LRFD with an average ratio of 0.86 for columns with $\lambda_c \leq 1.1$ and an average ratio of 0.60 for columns with $\lambda_c \geq 1.1$. This was attributed to the fact that the proposed method assumes higher factor of safety for column buckling.

For Group 2 sections, the d_w/t_w ratio is varied from $1.7(E/F_y)^{1/2}$ to $2.0(E/F_y)^{1/2}$ whereas the A_f/A_w ratio is varied from 1 to 4. Column design curves determined by the proposed method are compared to the Euro-LRFD in Figure 13. Comparison shows that the ratio of design load computed by the proposed method to that computed by the Euro-LRFD is neared from 0.86 for columns with $\lambda_c \leq 1.1$ to 0.7 for columns with $\lambda_c \geq 1.1$.

For Group 3 columns, the C/t_f ratio is varied from $0.7(E/F_y)^{1/2}$ to $1.15(E/F_y)^{1/2}$, d_w/t_w ratio is varied from $1.7(E/F_y)^{1/2}$ to $2(E/F_y)^{1/2}$,whereas A_f/A_w is varied from 0.5 to 2.0. Results depicted in Fig. 15 showed that the proposed method is conservative compared to Euro-LRFD in all cases with an average ratio of 0.75 in the inelastic buckling range and 0.5 in the elastic buckling range.

9. Summary and Conclusions:

In this work, a proposed design method for the design of columns with slender plate elements is established based on the LRFD approach. Columns are classified into three Groups, Group 1: columns with slender unstiffened plate elements, Group 2: columns with slender stiffened plate elements and Group 3: columns with slender stiffened and unstiffened plate elements. A finite element model is constructed for axially loaded columns covering the three Groups of slender sections. The critical load obtained from stability analysis incorporating material and geometric nonlinearities and geometric imperfections is compared to the design compressive stress adopted by the AISC-LRFD and Euro-Code3 specifications. The comparison shows that the effective width concept adopted in the Euro-Code3 to account for local plate buckling provides a good representation for buckling of columns with thin-walled plate elements. On the other hand, it is shown that the AISC greatly underestimates the buckling resistance of columns with slender unstiffened plate elements having high flat width-to-thickness ratio. Therefore, the proposed method is established based on the effective area approach adopted in the Euro-Code3 and ECP-ASD specifications. Direct comparison of column design curves determined by the proposed approach with that adopted in Euro-Code3 specifications, showed that the proposed method is always conservative compared to the Euro-LRFD specifications. Comparison with AISC-LRFD showed that the proposed method is conservative for Group 1 sections with $A_f/A_w \geq 0.4$ and $C/t_f \leq 0.85(E/F_y)^{1/2}$ and for Group 3 sections with $C/t_f \leq (E/F_y)^{1/2}$. The proposed method is also conservative for Group 2 sections compared to the AISC-LRFD. This conclusion is considered satisfactory since it is illustrated that the AISC-LRFD underestimates the critical load especially for high C/t_f ratios. On the other hand, the ratio C/t_f seldom exceeds the limit $0.85(E/F_y)^{1/2}$ in practice.

Corresponding author
Mohamed A. A. El-Shaer
Civil and Construction Engineering Department, Higher Technological Institute, 10th of Ramadan City
ecg_group@yahoo.com

Appendix A: Comparison of Finite Element Results with AISC-LRFD, Euro-Code3 and Proposed method for Design of Thin-walled Columns.

Tables 1, 2 and 3 list the geometric configuration, slenderness ratio and steel grade of 144 column cases with sections Group 1, 2 & 3 respectively. The finite element critical load stress in t/cm^2 was listed with the design buckling stress in t/cm^2 obtained by the AISC-LRFD, Euro-Code3 and proposed method for each column.

Table 1 Comparison of Results for Group 1 Sections

C/t_f		Sections Composed of Mild Steel 37							
		20.71		25.14		29.58		34.02	
A_F/A_w		0.509		0.419		0.356		0.310	
L/i		48.74	97.48	51.26	102.52	53.66	107.32	55.95	111.9
F_{cr}	FE	1.912	1.327	1.887	1.240	1.906	1.159	1.956	1.049
	AISC	1.650	1.211	1.451	1.074	1.253	0.945	0.983	0.775
	Euro	1.686	1.159	1.607	1.078	1.557	1.015	1.524	0.962
	Propos	1.565	1.010	1.481	0.893	1.429	0.796	1.395	0.723
C/t_f		Sections Composed of Steel 44							
		19.17		24.65		30.12		35.60	
A_F/A_w		0.509		0.396		0.324		0.274	
L/i		48.74	97.48	52.07	104.14	55.19	110.38	58.15	116.36
F_{cr}	FE	2.243	1.429	2.195	1.297	2.229	1.171	1.881	0.997
	AISC	1.893	1.318	1.589	1.126	1.230	0.916	0.899	0.719
	Euro	2.173	1.313	2.124	1.203	2.076	1.108	2.029	1.024
	Propos	1.789	1.030	1.665	0.857	1.596	0.747	1.553	0.667
C/t_f		Sections Composed of Steel 52							
		20.529		25.359		30.190		35.021	
A_F/A_w		0.419		0.339		0.285		0.246	
L/i		51.25	102.5	54.41	108.82	51.25	102.5	54.41	108.82
F_{cr}	FE	2.814	1.458	2.796	1.318	2.814	1.458	2.796	1.318
	AISC	2.070	1.319	1.674	1.117	2.070	1.319	1.674	1.117
	Euro	2.609	1.319	2.533	1.203	2.609	1.319	2.533	1.203
	Propos	2.075	0.894	1.962	0.771	2.075	0.894	1.962	0.771

Table 2 Comparison of Results for Group 2 Sections

d_w/t_w		Sections Composed of Mild Steel 37							
		45.85		50.29		54.72		59.16	
A_F/A_w		0.788		0.864		0.940		1.017	
L/i		44.28	88.56	43.51	87.02	44.28	88.56	43.51	87.02
F_{cr}	FE	2.010	1.488	1.976	1.516	2.010	1.488	1.976	1.516
	AISC	1.855	1.395	1.834	1.413	1.855	1.395	1.834	1.413
	Euro	1.900	1.347	1.877	1.355	1.900	1.347	1.877	1.355
	Propos	1.791	1.278	1.761	1.276	1.791	1.278	1.761	1.276
d_w/t_w		Sections Composed of Steel 44							
		43.818		49.295		54.772		60.249	
A_F/A_w		0.813		0.915		1.017		1.118	
L/i		44.01	88.02	43.07	86.14	44.01	88.02	43.07	86.14
F_{cr}	FE	2.351	1.634	2.303	1.676	2.351	1.634	2.303	1.676
	AISC	2.130	1.536	2.094	1.564	2.130	1.536	2.094	1.564
	Euro	2.201	1.495	2.172	1.515	2.201	1.495	2.172	1.515
	Propos	2.045	1.360	2.004	1.364	2.045	1.360	2.004	1.364
d_w/t_w		Sections Composed of Steel 52							
		45.89		50.72		55.55		60.38	
A_F/A_w		0.966		1.067		1.169		1.271	
L/i		42.67	85.34	41.97	83.94	41.38	82.76	40.89	81.78
F_{cr}	FE	2.964	1.926	2.925	1.969	2.917	2.005	2.936	2.036
	AISC	2.604	1.802	2.576	1.820	2.554	1.829	2.537	1.837
	Euro	2.693	1.703	2.671	1.726	2.654	1.744	2.642	1.759
	Propos	2.481	1.447	2.454	1.472	2.434	1.493	2.421	1.510

Table 3 Comparison of Results for Sections Group 3

d_w/t_w		Sections Composed of Mild Steel 37															
		45.85				50.29				54.72				59.16			
C/t_f		20.7	25.1	29.5	34.0	20.7	25.1	29.5	34.0	20.7	25.1	29.5	34.0	20.7	25.1	29.5	34.0
A_F/A_w		0.56	0.47	0.39	0.34	0.62	0.51	0.43	0.38	0.67	0.56	0.47	0.41	0.73	0.60	0.51	0.44
L/i		47.5	49.9	52.1	54.2	46.6	48.7	50.8	52.8	45.7	47.7	49.6	51.5	44.9	46.9	48.7	50.5
F_{cr}	FE	1.836	1.792	1.782	1.767	1.804	1.724	1.701	1.693	1.762	1.674	1.639	1.618	1.726	1.635	1.592	1.569
	AISC	1.659	1.459	1.259	0.988	1.657	1.465	1.265	0.992	1.632	1.455	1.270	0.995	1.611	1.433	1.258	0.998
	Euro	1.626	1.535	1.483	1.446	1.583	1.488	1.428	1.385	1.548	1.445	1.379	1.335	1.519	1.408	1.336	1.288
	Propos	1.504	1.411	1.364	1.316	1.455	1.356	1.292	1.251	1.415	1.307	1.238	1.194	1.382	1.267	1.194	1.143
L/i		95	99.8	104.1	108.4	93.2	97.4	101.6	105.6	91.4	95.4	99.2	103	89.8	93.8	97.4	101
F_{cr}	FE	1.369	1.287	1.207	1.090	1.405	1.326	1.245	1.122	1.435	1.327	1.183	1.046	1.472	1.328	1.191	1.061
	AISC	1.235	1.098	0.966	0.790	1.255	1.117	0.982	0.803	1.273	1.133	0.997	0.813	1.276	1.147	1.009	0.822
	Euro	1.160	1.077	1.018	0.967	1.158	1.078	1.017	0.967	1.158	1.074	1.013	0.966	1.156	1.068	1.005	0.958
	Propos	1.000	0.884	0.794	0.720	0.990	0.876	0.790	0.716	0.981	0.865	0.780	0.712	0.972	0.855	0.771	0.706
d_w/t_w		Sections Composed of Steel 44															
		43.818				49.295				54.772				60.249			
C/t_f		19.2	24.6	30.1	35.6	19.2	24.6	30.1	35.6	19.2	24.6	30.1	35.6	19.2	24.6	30.1	35.6

A_F/A_w		0.583	0.454	0.371	0.314	0.583	0.454	0.371	0.314	0.583	0.454	0.371	0.314	0.583	0.454	0.371	0.314
L/i		47.17	50.20	53.04	55.73	47.17	50.20	53.04	55.73	47.17	50.20	53.04	55.73	47.17	50.20	53.04	55.73
F_{cr}	FE	2.135	2.061	2.018	1.908	2.135	2.061	2.018	1.908	2.135	2.061	2.018	1.908	2.135	2.061	2.018	1.908
	AISC	1.907	1.602	1.239	0.904	1.907	1.602	1.239	0.904	1.907	1.602	1.239	0.904	1.907	1.602	1.239	0.904
	Euro	1.988	1.877	1.810	1.767	1.988	1.877	1.810	1.767	1.988	1.877	1.810	1.767	1.988	1.877	1.810	1.767
	Propos	1.702	1.563	1.486	1.437	1.702	1.563	1.486	1.437	1.702	1.563	1.486	1.437	1.702	1.563	1.486	1.437
L/i		94.34	100.4	106.1	111.5	94.34	100.4	106.1	111.5	94.34	100.4	106.1	111.5	94.34	100.4	106.1	111.5
F_{cr}	FE	1.493	1.369	1.238	1.051	1.493	1.369	1.238	1.051	1.493	1.369	1.238	1.051	1.493	1.369	1.238	1.051
	AISC	1.359	1.163	0.944	0.729	1.359	1.163	0.944	0.729	1.359	1.163	0.944	0.729	1.359	1.163	0.944	0.729
	Euro	1.363	1.243	1.149	1.071	1.363	1.243	1.149	1.071	1.363	1.243	1.149	1.071	1.363	1.243	1.149	1.071
	Propos	1.036	0.856	0.741	0.662	1.036	0.856	0.741	0.662	1.036	0.856	0.741	0.662	1.036	0.856	0.741	0.662
d_w/t_w		**Sections Composed of Steel 52**															
		45.89				50.72				55.55				60.38			
C/t_f		20.53	25.36	30.19	35.02	20.53	25.36	30.19	35.02	20.53	25.36	30.19	35.02	20.53	25.36	30.19	35.02
A_F/A_w		0.570	0.462	0.388	0.334	0.570	0.462	0.388	0.334	0.570	0.462	0.388	0.334	0.570	0.462	0.388	0.334
L/i		47.43	49.97	52.38	54.69	47.43	49.97	52.38	54.69	47.43	49.97	52.38	54.69	47.43	49.97	52.38	54.69
F_{cr}	FE	2.507	2.432	2.305	2.148	2.507	2.432	2.305	2.148	2.507	2.432	2.305	2.148	2.507	2.432	2.305	2.148
	AISC	2.093	1.709	1.237	0.935	2.093	1.709	1.237	0.935	2.093	1.709	1.237	0.935	2.093	1.709	1.237	0.935
	Euro	2.294	2.181	2.109	2.060	2.294	2.181	2.109	2.060	2.294	2.181	2.109	2.060	2.294	2.181	2.109	2.060
	Propos	1.834	1.695	1.611	1.555	1.834	1.695	1.611	1.555	1.834	1.695	1.611	1.555	1.834	1.695	1.611	1.555
L/i		94.86	99.94	104.8	109.4	94.86	99.94	104.8	109.4	94.86	99.94	104.8	109.4	94.86	99.94	104.8	109.4
F_{cr}	FE	1.649	1.511	1.323	1.113	1.649	1.511	1.323	1.113	1.649	1.511	1.323	1.113	1.649	1.511	1.323	1.113
	AISC	1.438	1.216	0.949	0.755	1.438	1.216	0.949	0.755	1.438	1.216	0.949	0.755	1.438	1.216	0.949	0.755
	Euro	1.453	1.339	1.245	1.166	1.453	1.339	1.245	1.166	1.453	1.339	1.245	1.166	1.453	1.339	1.245	1.166
	Propos	0.894	0.759	0.670	0.606	0.894	0.759	0.670	0.606	0.894	0.759	0.670	0.606	0.894	0.759	0.670	0.606

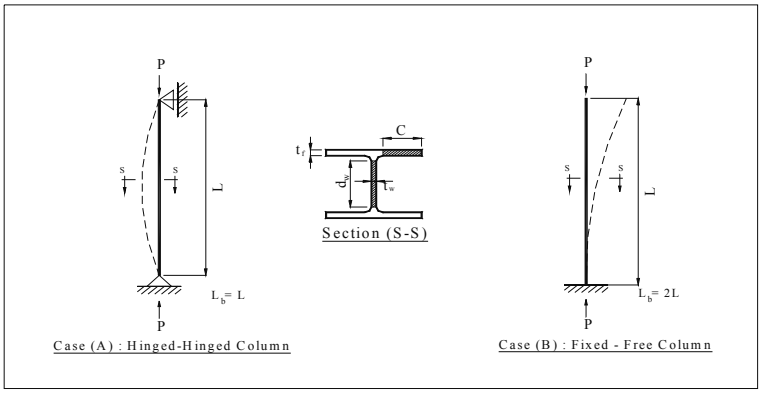

Figure 1 Geometric Configuration and Boundary Conditions

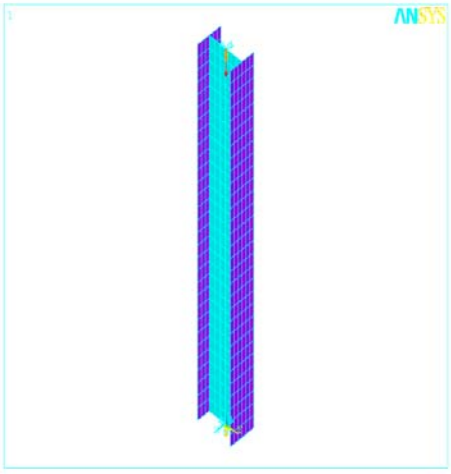

Figure 2 Finite Element Model of Axially Loaded Column

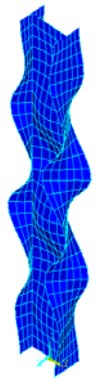

Figure 3 First Buckling Modes for Hinged-Hinged Column of Group 1

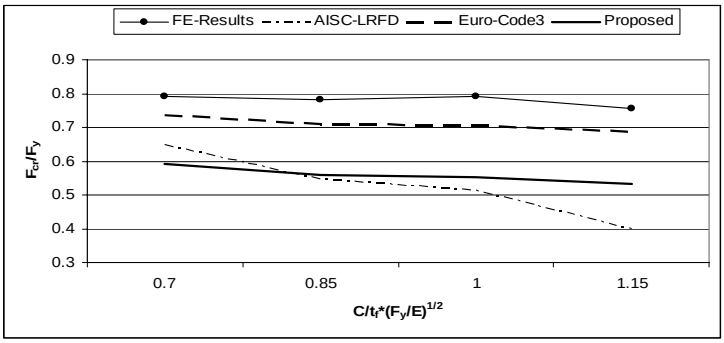

Figure 4 Comparison of results for short columns of Group 1 sections

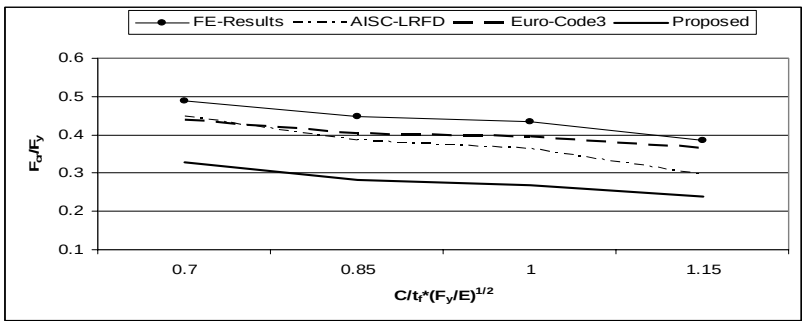

Figure 5 Comparison of results for medium columns of Group 1 sections

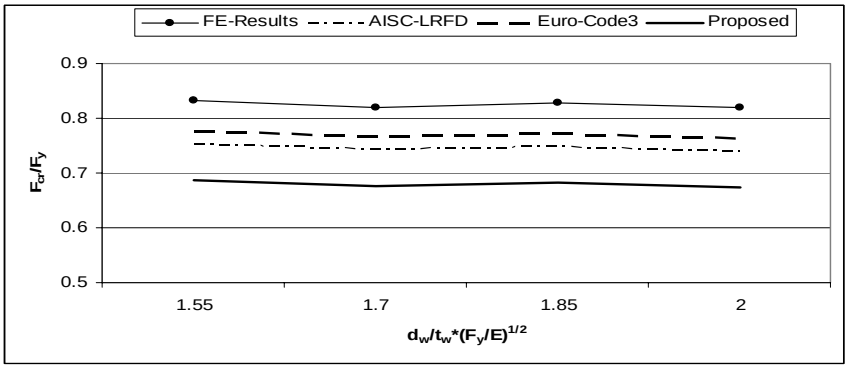

Figure 6 Comparison of Results for short columns of Group 2 sections

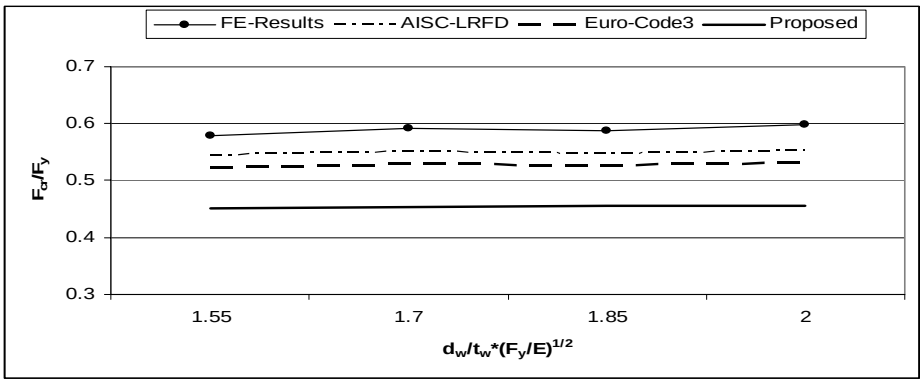

Figure 7 Comparison of Results for medium columns of Group 2 sections

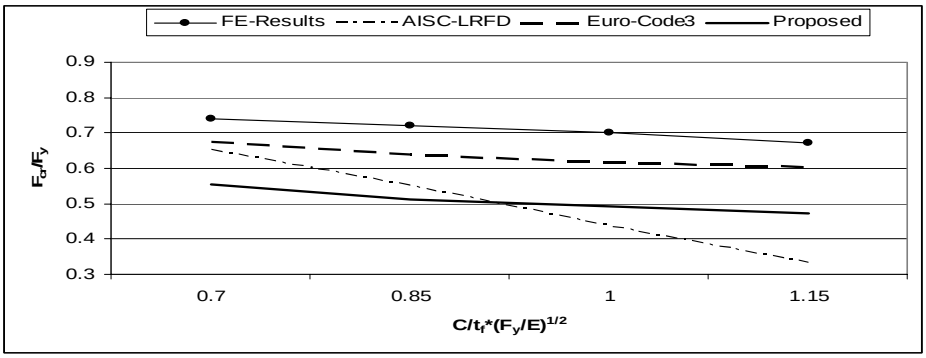

i) Group 3 with $d_w/t_w = 1.55(E/F_y)^{1/2}$

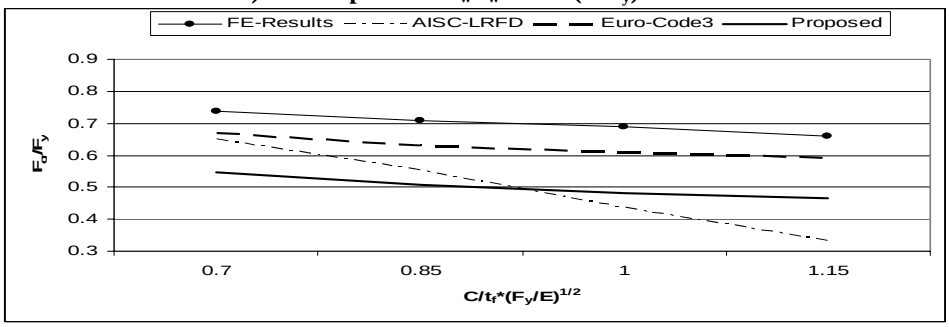

ii) Group 3 with $d_w/t_w = 1.70(E/F_y)^{1/2}$

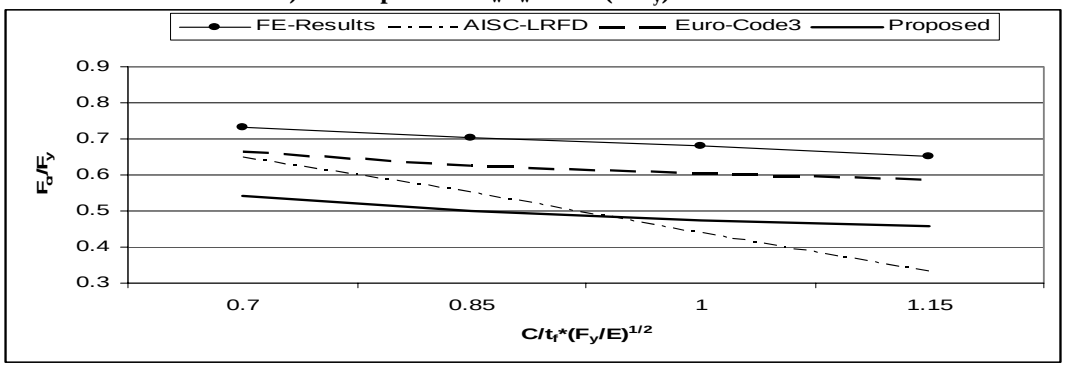

iii) Group 3 with $d_w/t_w = 1.85(E/F_y)^{1/2}$

Figure 8 Comparison of results for short columns of Group 3 sections

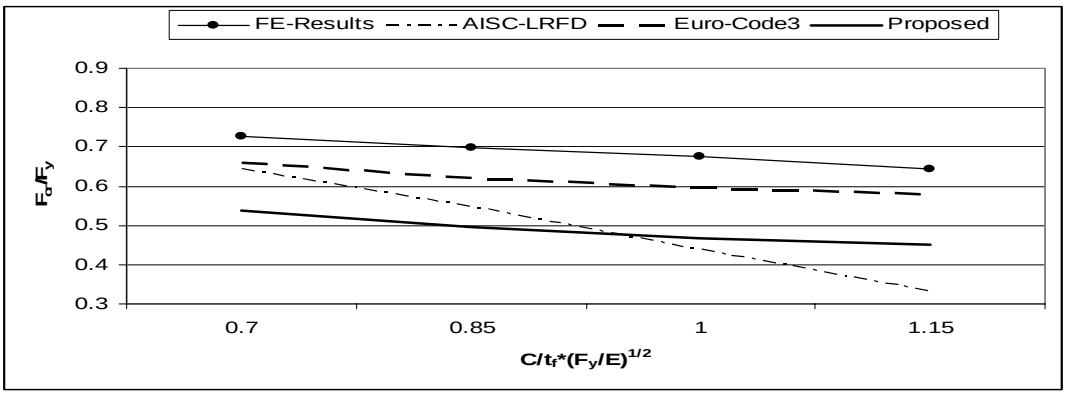

iv) Group 3 with $d_w/t_w = 2.0(E/F_y)^{1/2}$

Figure 8 (Continued)

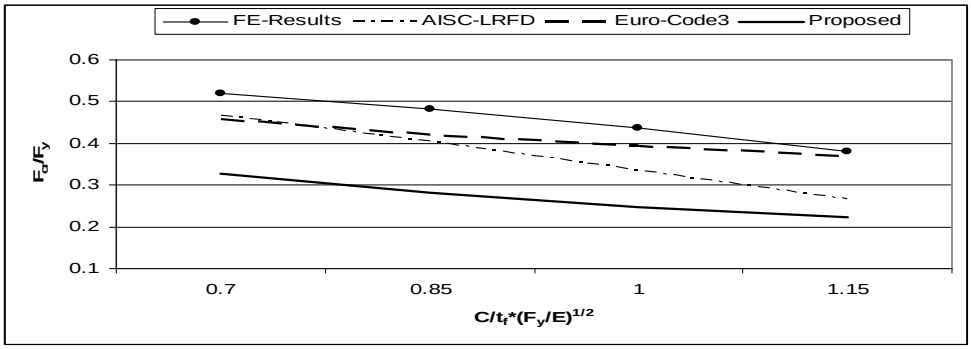

i) Group 3 with $d_w/t_w = 1.55(E/F_y)^{1/2}$

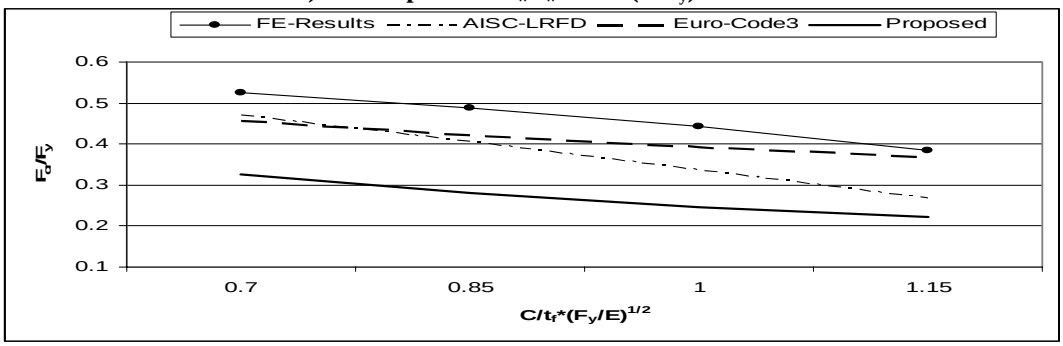

ii) Group 3 with $d_w/t_w = 1.70(E/F_y)^{1/2}$

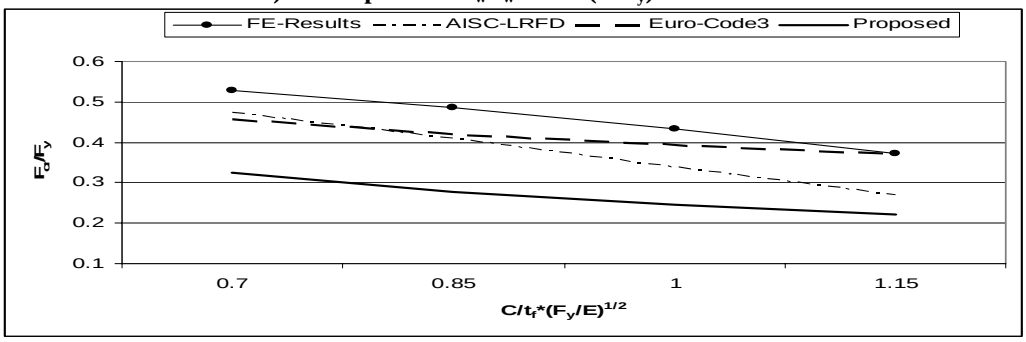

iii) Group 3 with $d_w/t_w = 1.85(E/F_y)^{1/2}$

Figure 9 Comparison of results for medium columns of Group 3 sections

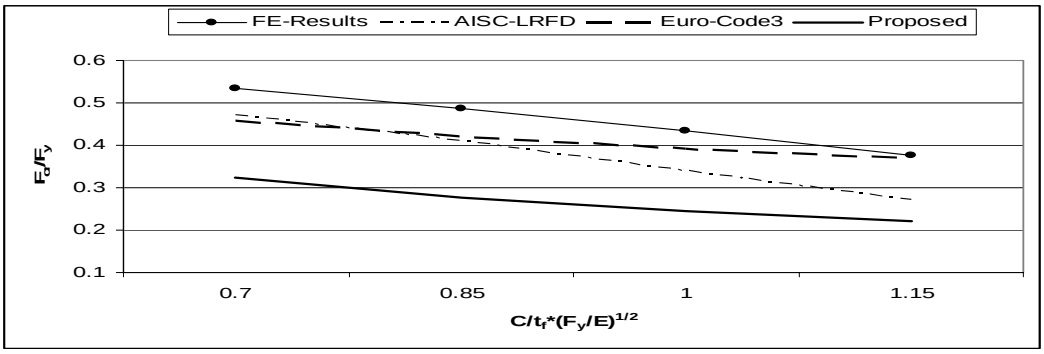

iv) Group 3 with $d_w/t_w = 2.0(E/F_y)^{1/2}$

Figure 9 (Continued)

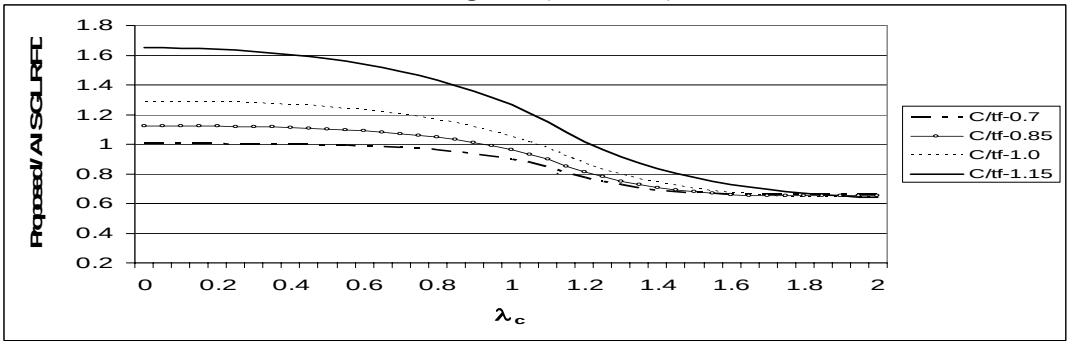

a) Af/Aw = 0.1

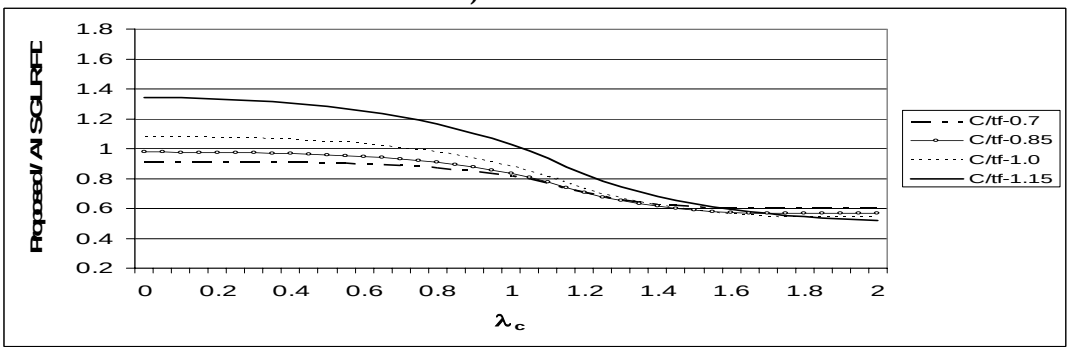

b) $A_f/A_w = 0.5$

Figure 10 Comparison of Proposed Column Design Curve (Eq 12) with AISC-LRFD Design Curve (Eq 2) for Group 1 Sections

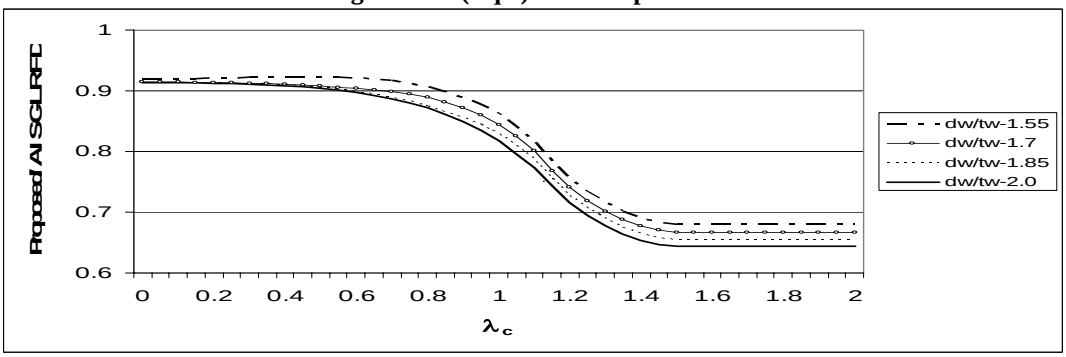

a) Af/Aw = 1

Figure 11 Comparison of Proposed Column Design Curve (Eq 12) with AISC-LRFD Design Curve (Eq 2) for Group 2 Sections

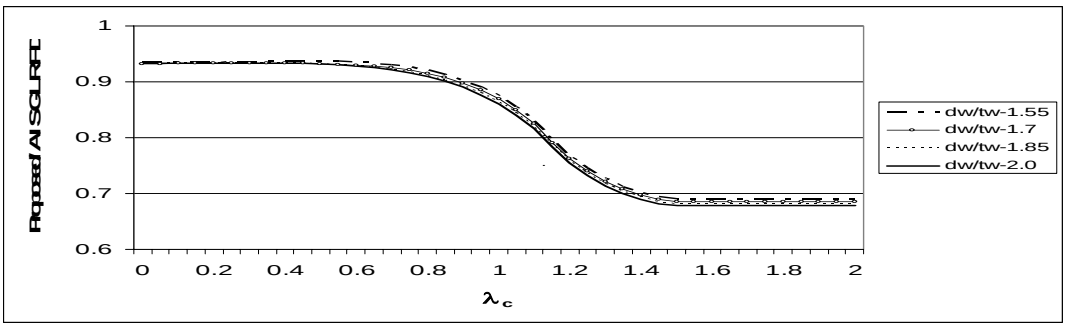

b) Af/Aw = 4

Figure 11 (Continued)

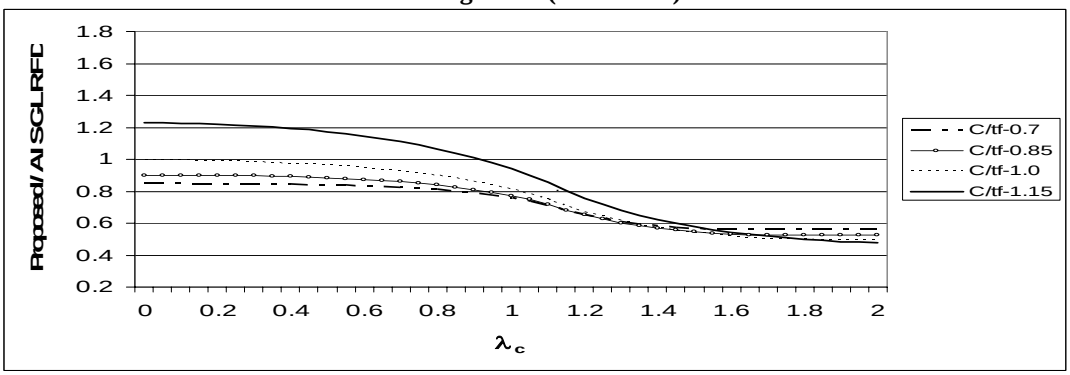

a) A_f/A_w = 0.5, $d_w/t_w = 1.7(E/F_y)^{1/2}$

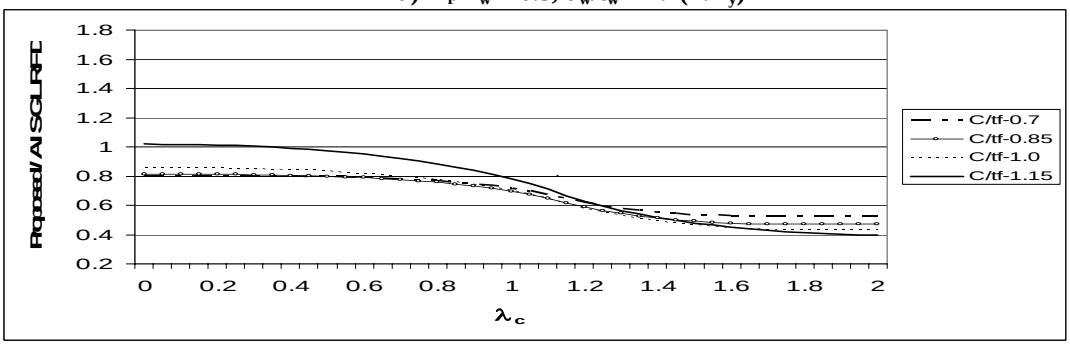

b) Af/Aw = 2.0, dw/tw = 1.7(E/Fy)1/2

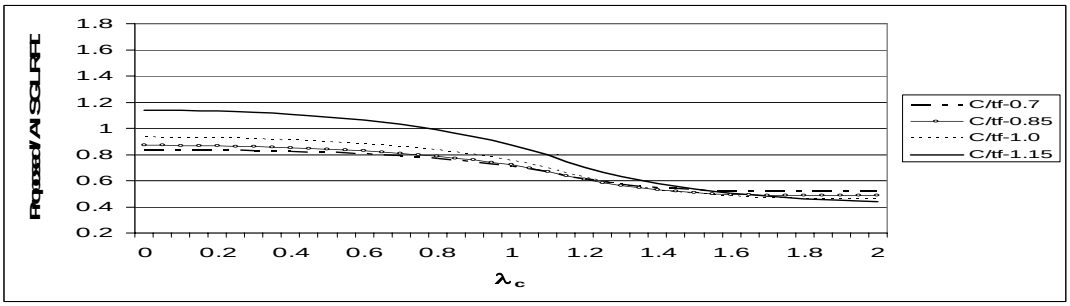

c) Af/Aw = 0.5, dw/tw = 2.0(E/Fy)1/2

Figure 12 Comparison of Proposed Design Curve (Eq 12) with AISC-LRFD Design Curve (Eq 2) for Group 3 Sections

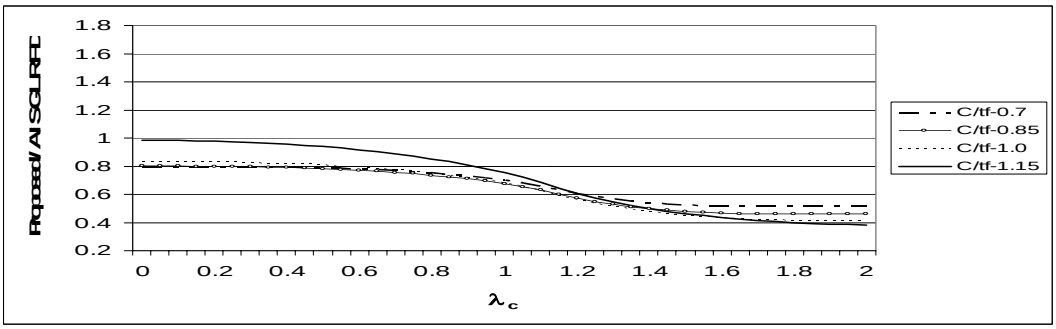

d) A_f/A_w = 2.0, $d_w/t_w = 2.0(E/F_y)^{1/2}$

Figure 12 (Continued)

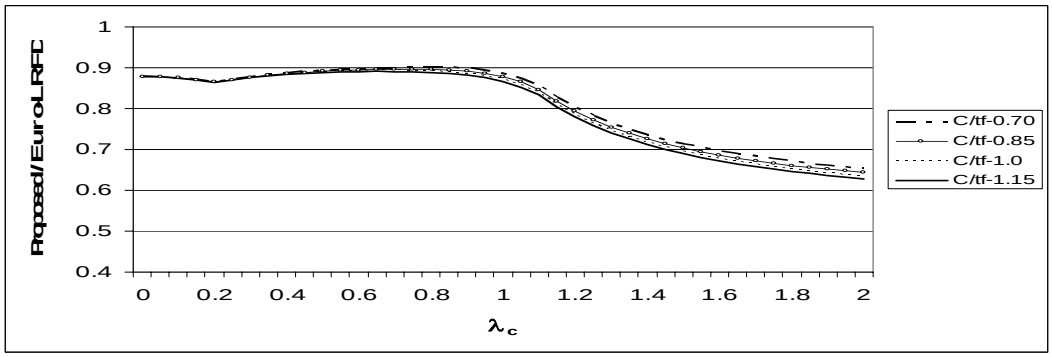

a) Af/Aw = 0.1

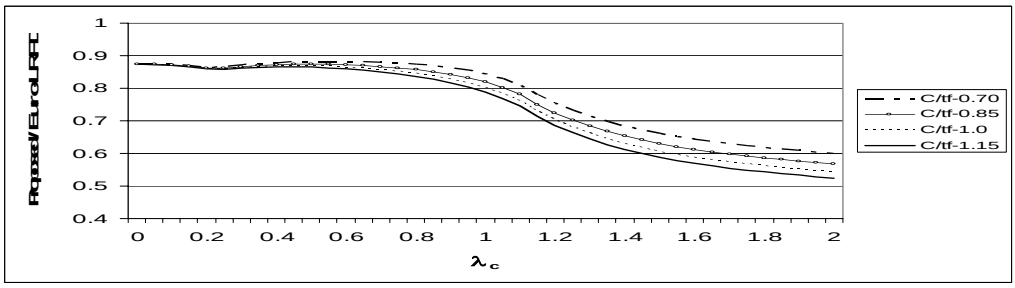

b) A_f/A_w = 0.50

Figure 13 Comparison of Proposed Column Design Curve (Eq12) with Euro-LRFD Design Curve (Eq 4) for Group 1 Sections

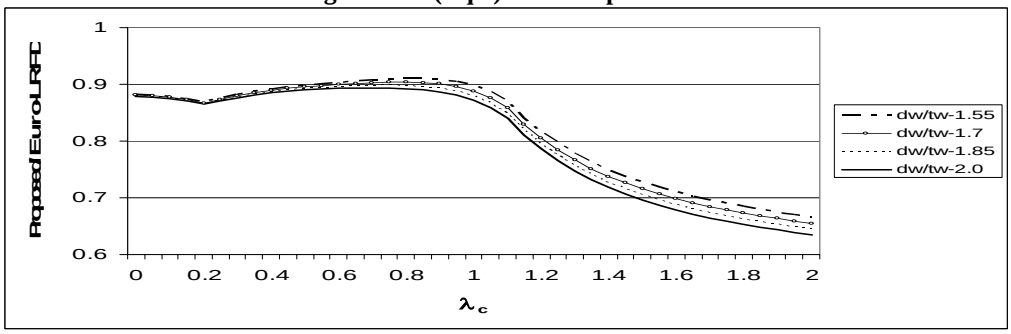

a) Af/Aw=1

Figure 14 Comparison of Proposed Column Design Curve (Eq 12) with Euro-LRFD Design Curve (Eq 4) for Group 2 Sections

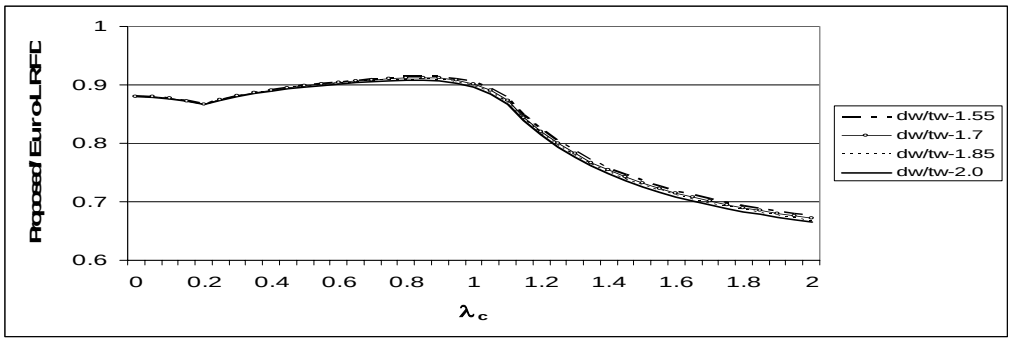

b) $A_f/A_w = 4$

Figure 14 (Continued)

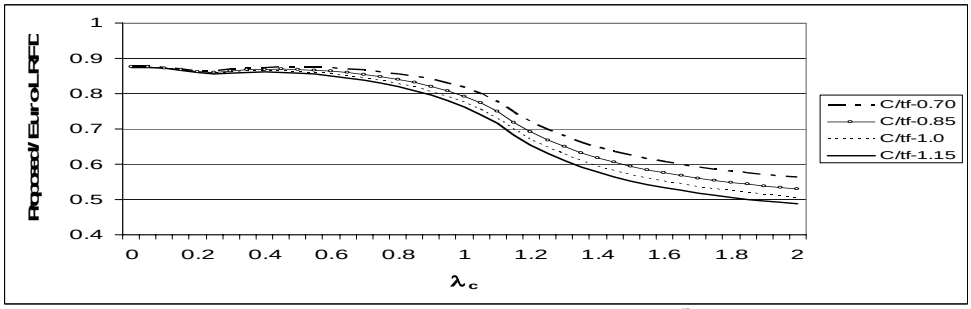

a) $A_f/A_w = 0.5$, $d_w/t_w = 1.7(E/F_y)^{1/2}$

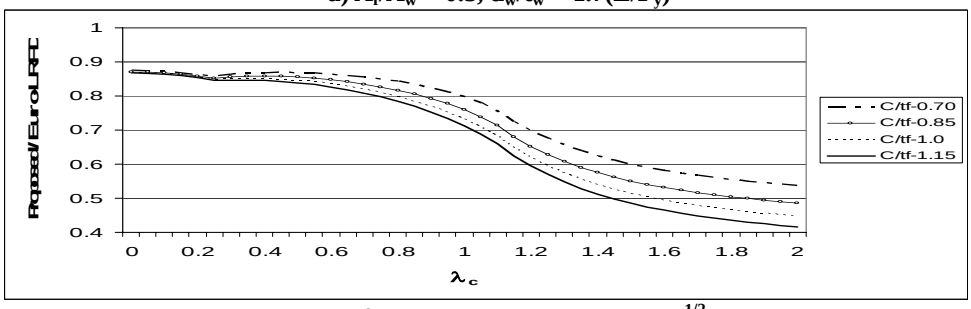

b) Af/Aw = 2.0, dw/tw = $1.7(E/Fy)^{1/2}$

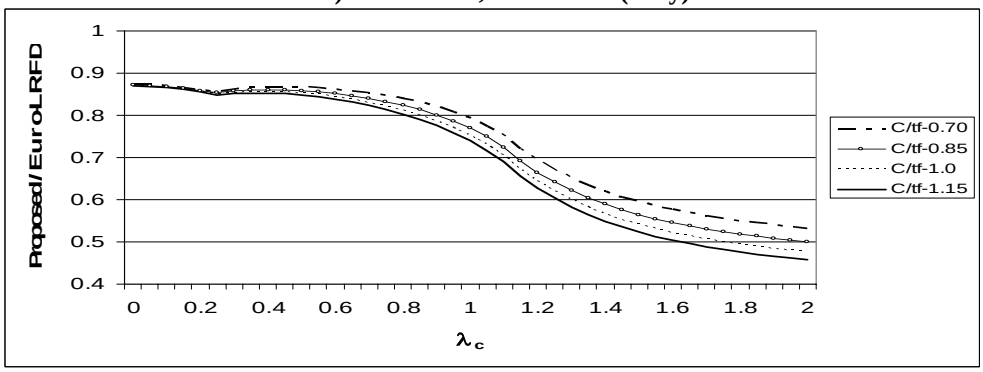

c) Af/Aw = 0.5, dw/tw = $2.0(E/Fy)^{1/2}$

Figure 15 Comparison of Proposed Design Curve (Eq 12) with Euro-LRFD Design Curve (Eq 4) for Group 3 Sections

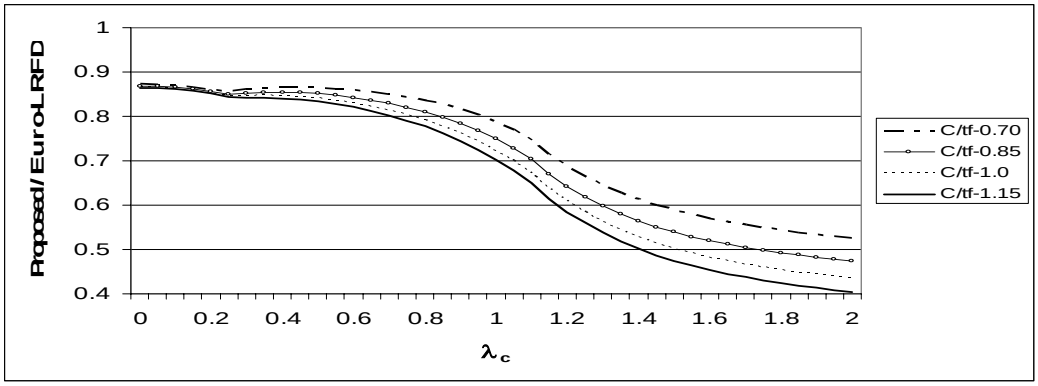

d) A_f/A_w = 2.0, $d_w/t_w = 2.0(E/F_y)^{1/2}$
Figure 15 (Continued)

References:

1- Salmon, C.G. and Johnson, J.E. (1996)." Steel Structures: Behavior and Design", Harper and Row Publishers, 4th Edition, 1996.
2- Timoshenko and Gere, "Theory of Elastic Stability", McGraw Hill, 3rd Edition, 1978
3- Dawson R.G. and Walker A.C.(1972)."Post-Buckling of Geometrically Imperfect Plates", Journal of Structural Division, ASCE Proceedings, 98(1).
4- Lind N.C., Ravindra M.K., and Schorn G. (1976). "Empirical Effective Width Formula", Journal of Structural Division, ASCE Proceedings, 102(9).
5- Horne M.R. and Narayanan R.(1977). "Design of Axially Loaded Stiffened Plates", Journal of Structural Division, ASCE Proceedings, 103(11).
6- Usami T., "Post-Buckling of Plates In Compression And Bending", Journal of structural division, ASCE proceedings, vol. 108, No. 3, Mar. 1982.
7- Lind N.C. (1978). "Numerical Buckling Analysis of Plate Assemblies", Journal of structural division, ASCE Proceedings, 104(2).
8- Sherbourne A.N. and Korol R.M. (1972). "Post-Buckling of Axially Compressed Plates", Journal of Structural Division, ASCE Proceedings, 98(10).
9- Dawe J.L. and Gilbert Y. Grondin(1985). "Inelastic Buckling of Steel Plates" Journal of structural division, ASCE Proceedings, 111(1):
10- Dawe J.L., Elgabry A.A., and Grondin G.Y., "Local Buckling of Hollow Structural Sections "Journal of structural division, ASCE proceedings, vol. 111, No. 5 May, 1985.
11- Hancock G.J. (1981). "Nonlinear Analysis of Thin Sections In Compression", Journal of structural division, ASCE Proceedings, 107(3).
12- Manual of Steel Construction, Load and Resistance Factor Design, Vol. 1, 2nd Edition 1994.
13- Yu, W.W. (1990). Cold-Formed Steel Design". John Wiley and sons, 2nd Edition, 1990.
14- Eurocode 3: Design of Steel Structures, Part 1.1 General rules and rules for buildings (together with United Kingdom National Application Document) DD ENV 1993-1-1:1992.
15- Egyptian Code of practice for Steel Construction and Bridges (Allowable Stress Design), Code no. Ecp (205), 1st Edition 2001, Edition 2008.
16- Egyptian Code of practice for Steel Construction (load and Resistance) factor Design (LRFD) (205) Ministerial Decree No. 359-2007 First Edition 2008.
17- Safar, S.S. and El-Shaer, M. (2002). "A Column Design Formula For Compact and Non-Compact Compression Members Using LRFD Method", Engineering. Res. Jour., Helwan University, Faculty of Engineering, Mataria, 81:39-56.
18- Chen, W.F. and Lui, E.M. (1987)."Structural Stability: Theory and Implementation", McGraw Hill,.
19- Brush,D.O. and Almorth, B.O. (1975). "Buckling of Bars, Plates and Shells", McGraw Hill, 1st Edition, New York, 1975.
20- Desalvo, G.J., and Gorman, R.W. (1989) "ANSYS User's Manual", Swanson Analysis Systems, , Houston, PA.
21- Bathe, K.J. (1996). "Finite Element Procedures", Prentice Hall, Englewood Cliffs, New Jersy,

10/24/2011